ISSN 1990-7931, Russian Journal of Physical Chemistry B, 2023, Vol. 17, No. 5, pp. 1069–1082. © Pleiades Publishing, Ltd., 2023.

STRUCTURE OF CHEMICAL COMPOUNDS, QUANTUM CHEMISTRY, SPECTROSCOPY

In Situ Physicochemical Assessment of Gallium Nitride Nanosheet Sensor Towards Gas Detecting: A DFT Study

B. Esfandiari[a], F. Mollaamin[b, *], M. Monajjemi[c, **], H. Aghaie[a], and K. Zare[a]

[a] *Department of Chemistry, Science and Research Branch, Islamic Azad University, Tehran, Iran*

[b] *Department of Food Engineering, Faculty of Engineering and Architecture, Kastamonu University, Kastamonu, Turkey*

[c] *Department of Chemical Engineering, Central Tehran Branch, Islamic Azad University, Tehran, Iran*

** e-mail: smollaamin@gmail.com*

*** e-mail: maj.monajjemi@iauctb.ac.ir*

Received May 30, 2023; revised June 14, 2023; accepted June 20, 2023

Abstract—This article aims to study the adsorption of hazardous gases of nitric oxide (NO), nitrogen dioxide (NO_2) and ammonia (NH_3) by using monolayer graphitic GaN nanosheet with the employing density functional theory (DFT). The changes of charge density have shown a more important charge transfer for hexagonal honeycomb nanosheet of gallium nitride (GaN) which acts as the electron acceptor while gas molecules act as the stronger electron donors through adsorption on the graphitic-like GaN surface. The adsorption of NO and NO_2 molecules introduced spin polarization in the GaN sheet, indicating that it can be employed as a magnetic gas sensor for NO and NO_2 sensing. The partial density of states (PDOS) graphs have explained that the NO and NO_2 states in GaN nanosheet, respectively, have more of the conduction band between −5 to −10 eV, while nitrogen and oxygen states have minor contributions. Ga sites in GaN nanosheet have higher interaction energy from Van der Waals' forces with gas molecules. GaN nanosheet represents having enough capability for adsorbing gases of NO, NO_2 and NH_3 through charge transfer from nitrogen atom and oxygen atom to the gallium element owing to intra-atomic and interatomic interactions.

Keywords: gas sensor, gallium nitride (GaN), NO, NO_2, NH_3, langmuir adsorption, DFT

DOI: 10.1134/S1990793123050196

INTRODUCTION

Sensor attributes can change the resistance of the graphene nanosheet once the gas molecules act like acceptors or donors of electrons. Generally gas sensors are largely approved with the properties such as high selectivity and sensitivity, low cost, small size, long working life, and resistant activity in the different environmental status [1–3]. Based on application of graphene as gas sensor in some works [4–6], it has been confirmed that the charge transfer diffused by adsorbing of gas molecules on the graphene surface might be considered to produce sensitive detectors.

Different usages of carbon nanocompunds, such as adsorbing of hydrogen, hazardous compounds, gas and designing the sensor instruments have been investigated [7–12]. Recently, many materials including carbon nanostructures have been designed and applied as adsorptive removal of environmental pollutant gases [13–15]. Thus, it is essential to make high-implement gas detectors for distinguishing hazardous gases. In addition, enough implanting of the carbon nanostructures with transition metals might enhance their adsorbing ability and adjust their adsorbing selectivity as the excellent dopant applicants. The gas sensors containing metal oxides have been used to recognize hazardous pollutant gases having most of gas sensing characteristics except accurate selectivity [16]. Their detecting mechanism usually deals with the chemical interaction between the gas molecule and the oxygen molecule adsorbed on the surface, because cross sensitivity among various analyte gas compounds is obvious in a metal oxide-based sensor instrument [17, 18]. For example, the reconnaissance of SO_2 and NO_2 molecules is prevented due to cross-interference when diffused in a mixed status from a static origin [19].

Recently, two-dimensional nanomaterials with high surface and large like phosphorene, and silicene and have known efficient in gas detecting which can largely transfer the charge density between gas molecules and the substrates [20–23].

Semiconductor materials are mainly prepared from the elements in groups II to VI of the Periodic table [24]. The compound in the groups III–V, each atom of group III is bonded to four atoms of group V for attaining an octet in the valence band, when the

valence charge from an atom of group V transfers toward an atom of group III and cultivates partial ionic bonding to the crystal surface [25].

The GaN structure is one of the most discovered group III-nitride semiconductors which have been applied in different applications like electronic and optoelectronic devices, and sensor instruments [26–29]. Considering the prominent electronic properties of gallium nitride (GaN), it can be an appropriate case for gas sensing [30–36]. For instance, some studies have exhibited that $Ga_{12}N_{12}$ nanoclusters are capable for gas sensing of CO, NO, NO_2, and HCN gas molecules [37, 38]. Moreover, GaN nanostructures suggest firm action under different radiation and in space conditions at room-temperature and wide varieties of temperature and humidity as compared to metal-oxides [39]. In addition, it has been investigated that magnetic properties instead of electrical properties owing to the interaction between gas molecule and surface in the active compound, a graphitic-like GaN nanosheet could be applied as a largely selective magnetic gas detector for NO and NO_2 sensing [35, 36]. DFT computations have accomplished and indicated that GaN wurtzoids as an agent of GaN nanocrystals are appropriate for hydrogen detecting nanostructures. The nitrogen sites were discovered to have the function for the hydrogen sensing susceptibility. It's obvious that wurtzoids are bundles of capped (3, 0) nanotubes that build the wurtzite phase when they attain nanocrystal or bulk sizes [40].

Moreover, GaP has been investigated as a sensitive material for construction of anodically bonded cells for atomic detectors because of its properties containing optical transparency in the near "IR" and high thermal conductivity make it a notable option in sensor devices [41].

One-dimensional semiconductor nanowires often consist of polytypic structures, due to the coexistence of various crystal GaAs as the semiconductors by using the chemical vapor transport approach [42]. Concerning damaging impact of NO_2 on human health and environment makes NO_2 gas sensors and their state-of-the-art characteristics have been studied [43–45].

Ammonia "NH_3" which is an important ingredient of reactive nitrogen, participates in prevalent harmful impacts on health. Nitrogen atom in NH_3 helps to form the atmospheric aerosols which remain in the atmosphere for some days [46–48]. Moreover, "NH_3" is very crucial in biology and medicine as well as in environmental controlling equipment. Recently, GaP epitaxial nanowires have been investigated as efficient adsorption material of NH_3 detection with a simple device [49].

Therefore, this research wants to investigate the adsorption of hazardous gases of NO, NO_2 and NH_3 on the monolayer graphitic-like GaN nanosheet [50–52] employing density functional theory (DFT) to discover the adsorbing parameters of the GaN surface.

MATERIALS AND METHOD

In this work, the optimized calculations have been guided in the GaussView 6.06.16 [53] and computed by Gaussian 16, Revision C.01 [54] using the DFT method. The Perdew–Burke–Ernzerhof (PBE) functional with high-precision generalized gradient approximation (GGA) has been employed to achieve more authentic results [55]. Every simulated group contains a graphitic–like of length 25 Å with bond length of 1.95 Å for GaN with a single NO, NO_2 or NH_3 molecule adsorbed onto it (Fig. 1).

The charge transfer between adsorbates of NO, NO_2 and NH_3 and adsorbent of GaN nanosheet is calculated due to the Bader charge analysis [56]. This method can measure charge accumulation from the charge of each atom in the complex model. Finally, the total adsorption charge transfer can be obtained as formula: $\Delta Q_t = Q_2 - Q_1$, where Q_2 and Q_1 remark the charge of GaN and GaP after and before adoption of NO, NO_2 and NH_3. As a matter of fact, positive ΔQ_t indicates that electrons are transferred from gas molecules of NO, NO_2 and NH_3 to the surfaces of GaN and nanosheet, and the adsorbent acts as an electron acceptor [57, 58].

The adsorbing of NO, NO_2 and NH_3 gases on the surfaces of GaN nanosheet was defined by the theory "Langmuir" isotherm [59–61], which indicates the chemisorption between gas molecules and GaN surface. The adsorbates of NO, NO_2 and NH_3 molecules are maintained on the surface of GaN with "Langmuir" chemisorption (Fig. 1).

The changes of charge density analysis in the adsorption process has illustrated that GaN nanosheet shows the Bader charge of –1.382e, before adsorption of NO, NO_2 and NH_3, and –0.598e, –0.904e, –0.625e, after adsorption of NO, NO_2 and NH_3, respectively.

Therefore, the changes of charge density for "Langmuir" adsorption of NO, NO_2 and NH_3 on GaN surface alternatively are $\Delta Q_{NO \to GaN} = +0.784 > \Delta Q_{NH_3 \to GaN} = +0.757 > \Delta Q_{NO_2 \to GaN} = 0.478$.

The values of changes of charge density have shown a more important charge transfer for GaN which acts as the electron acceptor while gas molecules act as the stronger electron donors through adsorption on the graphitic-like GaN surface.

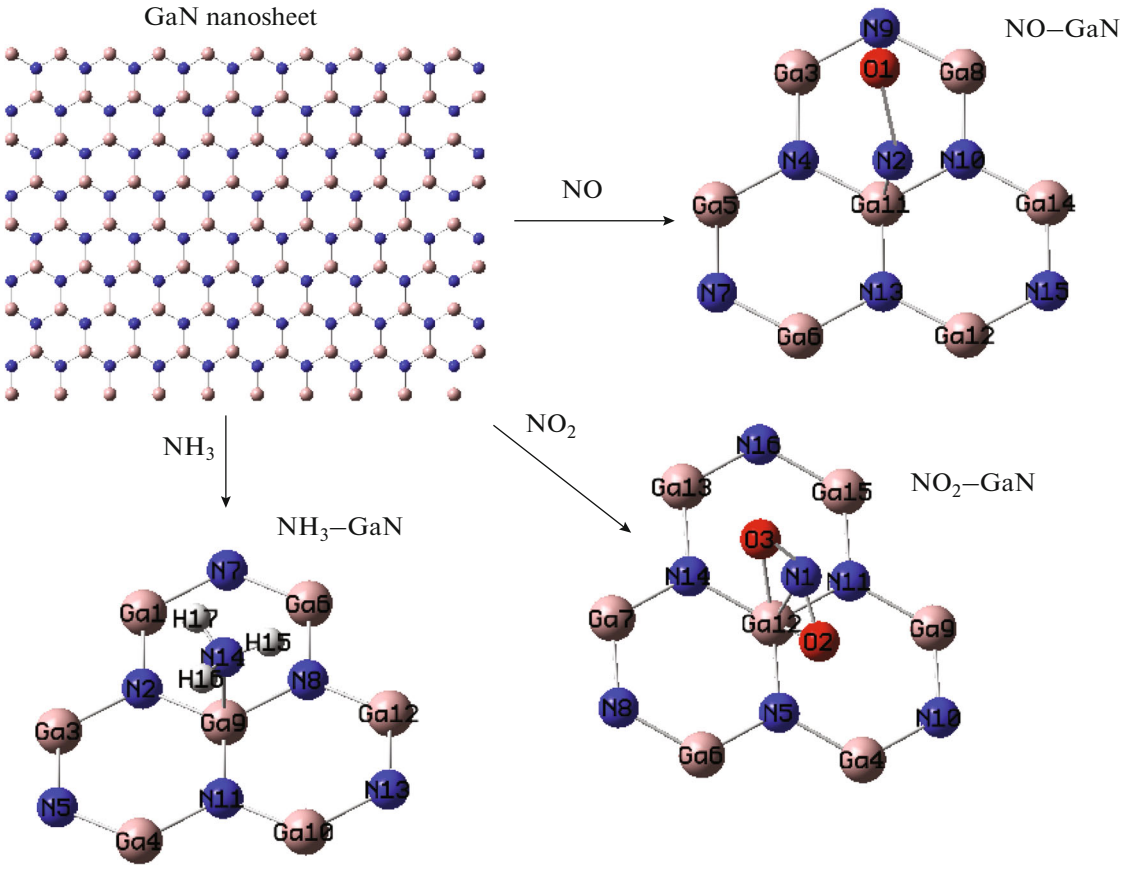

Fig. 1. "Langmuir" adsorption of NO, NO_2 and NH_3 onto GaN nanosheet.

For calculating the adsorption energy, the total energy of the NO, NO_2, NH_3 molecules and GaN surface should be computed. As it has been shown in Fig. 1, we have built a graphitic-like of length 25 Å with bond length of 1.95 Å for GaN. Then, we have tailored the spin-polarized DFT calculation with "ONIOM" model [62] accompanying the same force and energy convergence accuracy to the adsorption systems, with CAM-B3LYP [63] functional and with 6-311+G(d, p) [64] basis set for hydrogen, nitrogen, oxygen, and LANL2DZ for gallium in the adsorption sites for the first layer (high level). Second layer (medium level) has been considered on some gallium atoms and nitrogen atoms of GaN nanosheet, respectively, in the adsorption site due to semi-empirical methods. The third layer (low level) has been saved on the remained gallium atoms and also remained nitrogen atoms of GaN nanosheet with molecular mechanic force fields [62] as formula:

$$E_{\mathrm{ONIOM}} = E_{1st} + E_{2nd} + E_{3rd}.$$

To determine the most sensitive structure of gallium nitride (GaN) as the selective sensor for detecting gas molecules of NO, NO_2, NH_3, the binding energy of each system has been calculated. Therefore, we have found that the priority for selecting the surface binding of N-atom of NO, NH_3 and O-atom of NO_2 in adsorption site can be impacted by the existence of close atoms in the GaN surface. The simulated distribution functions of NO → GaN, NO_2 → GaN and NH_3 → GaN have illustrated that the created clusters lead to the bond lengths of N → Ga in NO → GaN (1.41 Å), O → Ga in NO_2 → GaN (2.43 Å) and N → Ga in NH_3 → GaN (2.19 Å) (Fig. 1).

Nuclear quadrupole resonance (NQR) method has been carried out for the complexes of NO, NO_2 and NH_3 adsorption on the graphitic-like GaN nanosheet. NQR method is based on the multipole enlargement in cartesian harmonies as the following equations:

$$V(r) = V(0) + \left[\left(\frac{\partial V}{\partial x_i}\right)_0 x_i\right] + \frac{1}{2}\left[\left(\frac{\partial^2 V}{\partial x_i x_j}\right)_0 x_i x_j\right] + \ldots \quad (1)$$

Then, after simplification the equation, there are only the second derivatives dependent on the same variable for the potential energy [65, 66]:

$$U = -\frac{1}{2}\int_D d^3 r \rho_r \left[\left(\frac{\partial^2 V}{\partial x_i^2}\right|_0 x_i^2\right)] = -\frac{1}{2}\int_D d^3 r \rho_r \left[\left(\frac{\partial E_i}{\partial x_i}\right|_0 x_i^2\right)] = -\frac{1}{2}\left(\frac{\partial E_i}{\partial x_i}\right|_0 \int_D d^3 r \left[\rho(r) x_i^2\right]. \quad (2)$$

There are two parameters which must be gotten from NQR method experiments; the quadrupole coupling constant, χ, and asymmetry parameter of the electric field gradient (EFG) tensor η:

$$\chi = e^2 Q q_{zz}/h, \quad (3)$$

$$\eta = q_{xx} - q_{yy}/ q_{zz}, \quad (4)$$

where q_{ii} are components of the EFG tensor at the quadrupole nucleus determined in the EFG principal axes system, Q the nuclear quadrupole moment, e the proton charge and h is the Planck's constant [67].

The electric potential (JC^{-1}) is a continuous function in space produced by an idealized point charge has $1/r$ potential:

$$V_E = \frac{1}{4\pi\varepsilon_0}\frac{Q}{r},$$

where Q (measured in coulombs) is the point charge, r is the distance from the charge and ε_0 is the permittivity of vacuum. Since the electric potential for a system of point charges is equal to the sum of the point charges' individual potentials, the calculations are done simply based on summation of potential fields which is scalar instead of summation of the electric fields which is vector and much more difficult that potential field. So,

$$V_E(r) = \frac{1}{4\pi\varepsilon_0}\sum_i \frac{q_i}{|r - r_i|},$$

where r is a point at which the potential is measured, r_i is a point at which the charge is $\neq 0$, and q_i is the charge at the point r_i. Finally, the potential of a continuous charge distribution $\rho(r)$ appears:

$$V_E(r) = \frac{1}{4\pi\varepsilon_0}\int_R \frac{\rho(r')}{|r - r'|} d^3 r',$$

where R is a region including all the points at which the charge density is $\neq 0$, r' is a point inside R, and $\rho(r')$ is the charge density at the point r' [68].

RESULTS AND DISCUSSION

In this investigation, gallium nitride (GaN) nanosheet have been investigated as the efficient surface because of their structural selectivity for adsorption of nitric oxide (NO), nitrogen dioxide (NO_2) and ammonia (NH_3). These experiments have been accomplished using spectroscopy analysis through some physical and chemical properties.

The electronic structures of NO and NO_2 adsorbed on the GaN nanosheet have been analyzed to simplify subsequent discussion for interfacial electronic properties using CAM-B3LYP/LANL2DZ, 6-311+G(d, p) basis sets. The graph of partial DOS (PDOS) has illustrated that the p states of N- and O-atoms during adsorption on the GaN nanosheet are dominant through the conduction band (Fig. 2). A distinct metallic feature can be observed in GaN nanosheet because of the strong interaction between the p states of N and the d state of Ga near the Fermi energy. Moreover, the existence of covalent features for these complexes has exhibited the identical energy amount and figure of the PDOS for the p orbitals of N, O and d orbitals of Ga (Fig. 2).

Figure 2a shows that the NO states in both of GaN nanosheet, respectively, have more contribution at the middle of the conduction band between −5 to −10 eV, while contribution of gallium sates are expanded, but nitrogen and oxygen states have minor contributions. In addition, Fig. 2b illustrates that the adsorption of NO_2 on GaN nanosheet has more contribution at the middle of the conduction band between −5 to −10 eV, while contribution of gallium are expanded, but nitrogen and oxygen states have minor contributions.

The results also approved by the partial density of states (PDOS) which have showed a certain charge association between GaN nanosheet and gas molecules of NO and NO_2.

In other words, N states in GaN nanosheet have less contribution. Thus, the above results exhibit that the cluster dominant of non-metallic and metallic features and a certain degree of covalent features can illustrate the increasing of the semiconducting direct band gap of gas molecules adsorbing on the GaN nanosheet.

As the EFG at the position of the nucleus in gas adsorbed on the gallium nitride nanosheet as the gas sensor is assigned by the valence electrons twisted in the special linkage with close nuclei of GaN nanosurface, the NQR method frequency at which transitions happen is particular for NO→ GaN, NO_2 → GaN, and NH_3 → GaN complexes (Table 1, Fig. 1).

In addition, in Fig. 3, it has been plotted the electric potential of NQR method versus Bader charge for elements of hydrogen, nitrogen, oxygen and gallium in the adsorption process of NO, NO_2, NH_3 on the GaN nanosheet using CAM-B3LYP/EPR-III, LANL2DZ, 6-311+G(d, p) level of theory.

In Fig. 3, it has been remarked the changes of electric potential for hydrogen, nitrogen, oxygen and gallium in the active site of Langmuir adsorption. In fact, it has been observed the effect of the binding between H, N, and O with gallium in the GaN nanosheet

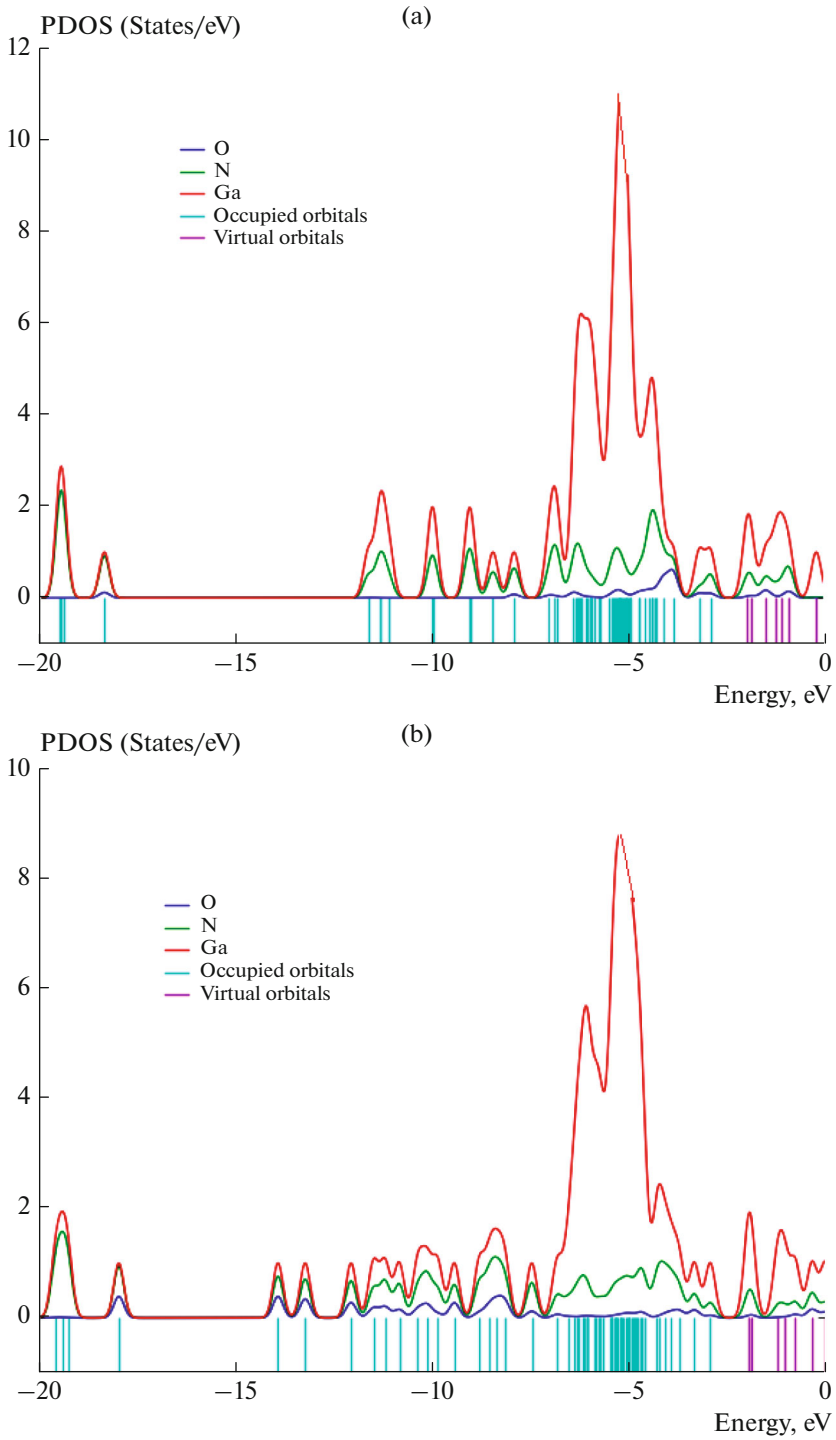

Fig. 2. PDOS adsorption of (a) NO → GaN and (b) NO_2 → GaN nanosheets.

during adsorbing NO, NO_2, NH_3 through resulted electric potential using NQR analysis (Fig. 3). It's obvious that the capability of GaN for detecting of NO, NO_2, NH_3 is fluctuated by their selectivity and sensitivity which can represent the efficiency of these surfaces as the promising sensors.

Isotropic (σ_{iso}) and anisotropy (σ_{aniso}) shielding tensors of nuclear magnetic resonance (NMR) spectroscopy for certain atoms in the active site of NO, NO_2 and NH_3 adsorbed on the GaN nanosheet (Fig. 1) through the formation of the binding between gas molecules and solid surfaces have been calculated

Table 1. The electric potential (E_p) and Bader charge (Q) for elements involving in the adsorption mechanism of NO, NO_2, NH_3 on the GaN nanosheet using CAM-B3LYP/EPR-III, 6-311+G(d, p) calculation extracted of NQR method

:Ö = Ṅ:→ GaN			:Ö: –Ṅ = Ö:→ GaN			H | H–N: → GaN | H		
Atom	Q	E_p	Atom	Q	E_p	Atom	Q	E_p
O1	–0.2246	–22.2691	N1	–0.2230	–18.2043	Ga1	0.2822	–146.59
N2	–0.2626	–18.2995	O2	–0.2686	–22.0279	N2	–0.475	–18.1517
Ga3	0.5194	–147.0664	O3	–0.2213	–21.9945	Ga3	0.2250	–146.608
N4	–0.5262	–18.2340	Ga4	0.34732	–147.21	Ga4	0.2448	–146.605
Ga5	0.4550	–147.089	N5	–0.4432	–18.1789	N5	–0.3370	–18.2079
Ga6	0.4560	–147.0976	Ga6	0.42893	–147.054	Ga6	0.2829	–146.589
N7	–0.4657	–18.2970	Ga7	0.35341	–147.183	N7	–0.3291	–18.1879
Ga8	0.5163	–147.0630	N8	–0.4313	–18.2753	N8	–0.4778	–18.1569
N9	–0.4684	–18.2961	Ga9	0.38506	–147.067	Ga9	0.6245	–146.646
N10	–0.5317	–18.2336	N10	–0.4326	–18.2994	Ga10	0.2323	–146.608
Ga11	0.5978	–147.2992	N11	–0.5487	–18.2298	N11	–0.4627	–18.1606
Ga12	0.4672	–147.0987	Ga12	0.9045	–147.234	Ga12	0.1992	–146.611
N13	–0.5280	–18.2393	Ga13	0.5788	–147.098	N13	–0.3379	–18.2106
Ga14	0.4607	–147.0861	N14	–0.4801	–18.1804	N14	–0.4815	–17.8981
N15	–0.4652	–18.2971	Ga15	0.5136	–147.016	H15	0.2739	–0.89106
			N16	–0.4626	–18.282	H16	0.2685	–0.89209
						H17	0.2676	–0.89065

using Gaussian 16, Revision C.01 and reported in Table 2 [54, 69].

It was observed the chemical shielding (ppm) of "NMR" curves versus atom type through adsorption of NO, NO_2, NH_3 onto GaN nanosheet (Figs. 1–4). The resulted graphs of "NMR" data in Fig. 4 have shown approximately the identical chemical shielding behavior of isotropic and anisotropy factors for NO → GaN nanosheet with several sharp peaks related to gallium atoms involving the adsorption site (Ga3, Ga5, Ga6, Ga8, Ga12, Ga14) (Fig. 4), NO_2 → GaN nanosheet with several sharp peaks related to gallium atoms involving the adsorption site (Ga4, Ga6, Ga7, Ga8, Ga9, Ga13, Ga15) (Fig. 4b), and NH_3 → GaN nanosheet with several sharp peaks related to gallium atoms corresponding the adsorption site (Ga1, Ga3, Ga4, Ga6, Ga9,Ga10, Ga12) (Fig. 4c). Although, in the "NMR" spectroscopy, it has been observed the remarkable peak around gallium atom in the GaN nanosheet through the adsorption procedure of gas molecules, there are some fluctuations in the chemical shielding behaviors of isotropic and anisotropy attributes.

Furthermore, the stability of complexes including gas adsorption on graphitic gallium nitride (GaN) nanosheet has been investigated through thermodynamic properties which define the reactions that gas molecules of (NO), nitrogen dioxide (NO_2), and ammonia (NH_3) endure in the gallium coordination sphere. Concerning adsorption process, the thermodynamic characters were evaluated for NO, NO_2, and NH_3 on the surfaces of graphitic gallium nitride (GaN) as the gas detectors which can be applicable as the selective sensors for these gases (Table 3).

The "IR" spectrums for adsorption of NO, NO_2, and NH_3 on the surfaces of GaN nanosheet have been reported in Fig. 5. The graphs of Fig. 5a has been observed in the frequency range between 50–500 cm^{-1} for the complexes of NO → GaN with a sharp peak around 200 cm^{-1}.

Figure 5b has shown the several strongest IR peaks of NO_2 → GaN cluster approximately between 200–1150 cm^{-1}. Besides, it has been seen the frequency sharp peaks of 850, 1150 cm^{-1} for NO_2 → GaN (Fig. 5b). Furthermore, the several strong frequency fluctuations for NH_3 → GaN nanosheet have been repre-

sented between 100–1200 cm^{-1} with a sharp peak around 1150 cm^{-1} for $NH_3 \rightarrow GaN$ complex (Fig. 5c).

In addition, the high amounts of the "Langmuir" adsorption isotherm graphs based on relative adsorption energy (ΔE^0_{ads}) has been evaluated for interactions between NO, NO_2, and NH_3 on the surfaces of GaN nanosheet with $R^2 = 0.9343$ (Fig. 6).

The adsorptive capacity of NO, NO_2, and NH_3 on the surfaces of GaN is approved by the ΔE^0_{ads} amounts as formula:

$$\Delta E^0_{ads} = \Delta E^0_{X\rightarrow GAN} - \left(\Delta E^0_X + \Delta E^0_{GaN}\right),$$

where X is NO, NO_2 or NH_3.

Table 3 has shown that the adsorbing of NO, NO_2, and NH_3 on the surfaces of GaN nanosheet must have both "physical" and "chemical" nature. All the measured relative adsorption energies (ΔE^0_{ads}) are almost identical, and exhibit the accord of the estimated data by all methods and the accuracy of the calculations (Fig. 6). In fact, Ga sites in GaN nanosheet have higher interaction energy from Van der Waals' forces with gas molecules including NO, NO_2 and NH_3 that can make them highly stable.

In the case of adsorption, the area of the adsorbent becomes an additional thermodynamic variable. A similar situation arises for the equilibria of gas phase, where a specification of gas molecule (NO, NO_2, and $NH_{3)}$ is necessary to define the thermodynamic system. The pertinent additional intensive variable for the equilibria of gas molecule of NO, NO_2, and NH_3 is surface tension; similarly, the spreading pressure becomes an additional intensive variable for adsorption equilibria (Table 3 and Fig. 6).

From Fig. 6, ΔE^0_{ads} may depend on the interactions between the gas molecules of NO, NO_2, and NH_3 and the GaN surfaces. In fact, comparison to ΔE^0_{ads}, it is allocated a good accord ($R^2 = 0.9343$) among calculated results, and validity of the picked isotherm for the adsorption which produce the NO → GaN, $NO_2 \rightarrow GaN$, and $NH_3 \rightarrow GaN$ complexes.

In fact, GaN nanosheet seems possess enough efficiency for adsorption toxic gases of NO, NO_2 and NH_3 through charge transfer from nitrogen and oxygen to the gallium element due to intra-atomic and interatomic interactions.

In other words, the adsorbent is assumed to be thermodynamically inert; that is the change in a thermodynamic property of the adsorbent, such as internal energy, during an adsorption process at constant temperature is assumed to be negligible compared with the change in the same property for the adsorbing gas.

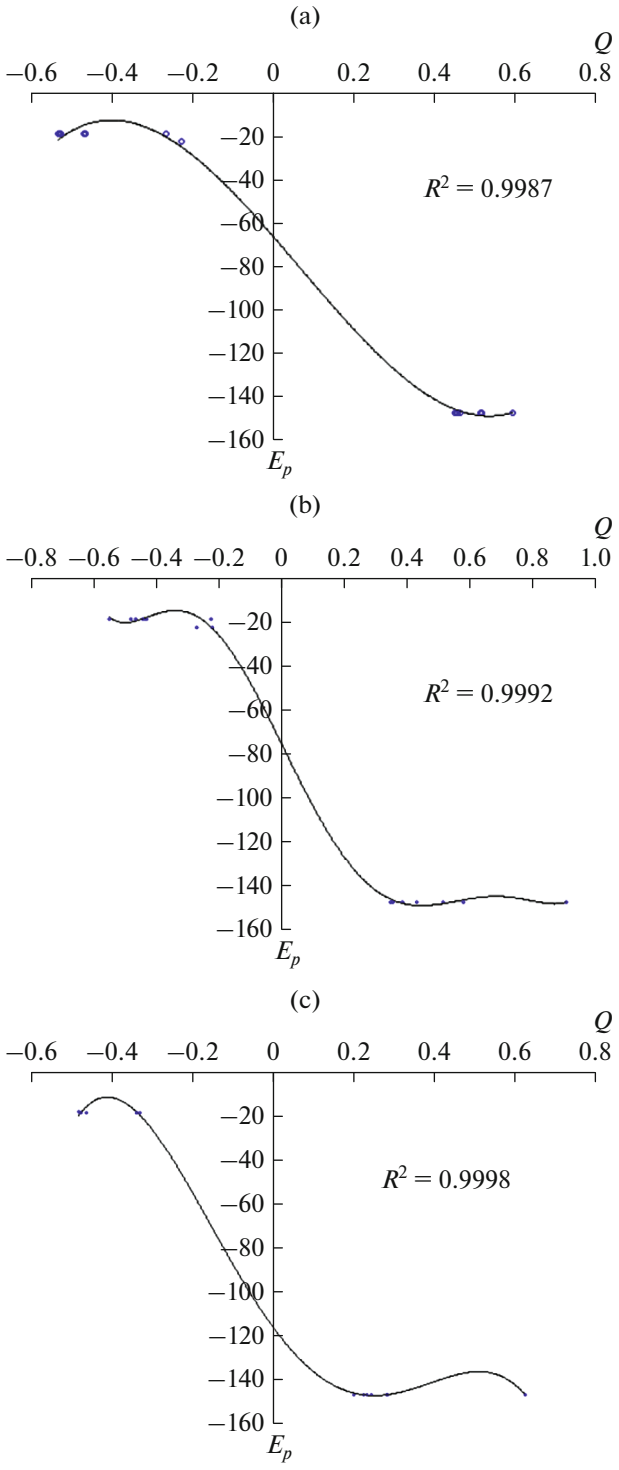

Fig. 3. The electric potential versus Bader charge through NQR calculation for adsorption clusters of (a) NO → GaN, (b) $NO_2 \rightarrow GaN$, and (c) $NH_3 \rightarrow GaN$ using CAM-B3LYP/EPR-III, LANL2DZ,6-31+G(*d*, *p*).

Based on frontier molecular orbital (FMO) theory, the LUMO and HOMO and the energy between them is the band gap of the adsorption system were computed. In fact, broad band gap diagram indicates that

Table 2. Data of nuclear magnetic resonance shielding tensors of isotropic (σ_{iso}) and anisotropy (σ_{aniso}) for selected atoms of NO, NO_2, NH_3 through adsorption on GaN nanosheet using CAM-B3LYP/EPR-III, 6-311+G (*d*, *p*) calculation

:Ö = Ṅ: → GaN			:Ö: –Ṅ = Ö: → GaN			H | H–Ṅ: → GaN | H		
Atom	σ_{iso}	σ_{aniso}	Atom	σ_{iso}	σ_{aniso}	Atom	σ_{iso}	σ_{aniso}
O1	4821.8747	13220.5719	N1	830.2777	6372.8449	Ga1	17626.0171	29573.0338
N2	737.8156	6496.7109	O2	1323.1030	6727.1193	N2	251.8641	354.4383
Ga3	2451.1239	29825.8262	O3	388.6740	3388.9901	Ga3	20005.1261	34085.0813
N4	1469.7502	3402.7758	Ga4	30814.9219	58182.6146	Ga4	17897.4195	29633.6318
Ga5	15553.2422	25607.9058	N5	1442.7706	13067.9649	N5	175.9060	629.9592
Ga6	11515.0022	20178.1529	Ga6	4010.8252	49917.8649	Ga6	17239.2677	29092.0179
N7	4314.9928	14492.9754	Ga7	26441.6944	114676.7699	N7	187.6651	394.6117
Ga8	2696.7458	37790.2395	N8	2338.2041	36057.6300	N8	232.8229	258.9451
N9	775.1003	2658.5011	Ga9	7173.4867	80927.3080	Ga9	16327.1187	23810.0447
N10	741.1297	3607.7969	N10	3879.4503	45938.3647	Ga10	18576.5314	30716.4928
Ga11	109.3018	2065.2926	N11	950.1517	4548.8274	N11	234.2999	503.8588
Ga12	3361.2055	10569.2187	Ga12	1439.0401	3651.1223	Ga12	19557.5661	33305.4682
N13	1448.2707	3249.5646	Ga13	18631.5643	74813.8800	N13	129.2701	618.9554
Ga14	7061.5546	16864.5428	N14	887.1812	9987.7736	N14	295.8192	25.3839
N15	150.5372	3369.7321	Ga15	15303.0265	23988.9456	H15	34.4223	13.4819
			N16	159.5638	5975.1969	H16	37.1167	14.4223
						H17	37.8487	18.8085

σ_{iso}—isotropic chemical-shielding, σ_{aniso}—anisotropic chemical-shielding: $\sigma_{iso} = \frac{\sigma 33 + \sigma 22 + \sigma 11}{3}$; $\sigma_{aniso} = \sigma 33 - \frac{\sigma 22 + \sigma 11}{2}$.

Table 3. The thermodynamic character of NO, NO_2 and NH_3 adsorbed on the GaN nanosheet as the selective gas sensors

Compound	$\Delta E^0 \times 10^{-4}$, kcal/mol	$\Delta E^0_{ads} \times 10^{-4}$, kcal/mol	$\Delta H^0 \times 10^{-4}$, kcal/mol	$\Delta G^0 \times 10^{-4}$, kcal/mol	S^0, cal/K mol	Dipole moment, D
Ga–N	–21.4958	–	–21.4957	–21.4998	137.460	0.6307
NO	–8.0017	–	–8.0016	–8.0031	48.968	0.2376
NO_2	–12.6298	–	–12.6298	–12.6315	57.792	0.2323
NH_3	–3.5437	–	–3.5436	–3.5450	48.176	2.1281
NO → GaN	–863.1604	–833.6629	–863.1604	–863.1644	133.724	4.8379
NO_2 → GaN	–867.7891	–833.6635	–867.7890	–867.7931	135.598	4.4976
NH_3 → GaN	–859.3971	–834.3576	–859.3970	–859.4014	145.511	5.0153

there is less conductivity [70–72]. The LUMO, HOMO, band energy gap (ΔE) and other quantities distributions of NO, NO_2, and NH_3 on the surfaces of GaN nanosheets as the gas detector systems denote that the gas adsorption procedure scatters the electrons of the system (Table 4).

The energy gap between HOMO and LUMO has represented the transporting of molecular electrical characters [73–76]. On the other hand, the difference between HOMO and LUMO has exhibited that the effect of the adsorption process on the electronic behavior of NO, NO_2, and NH_3 on the surfaces of

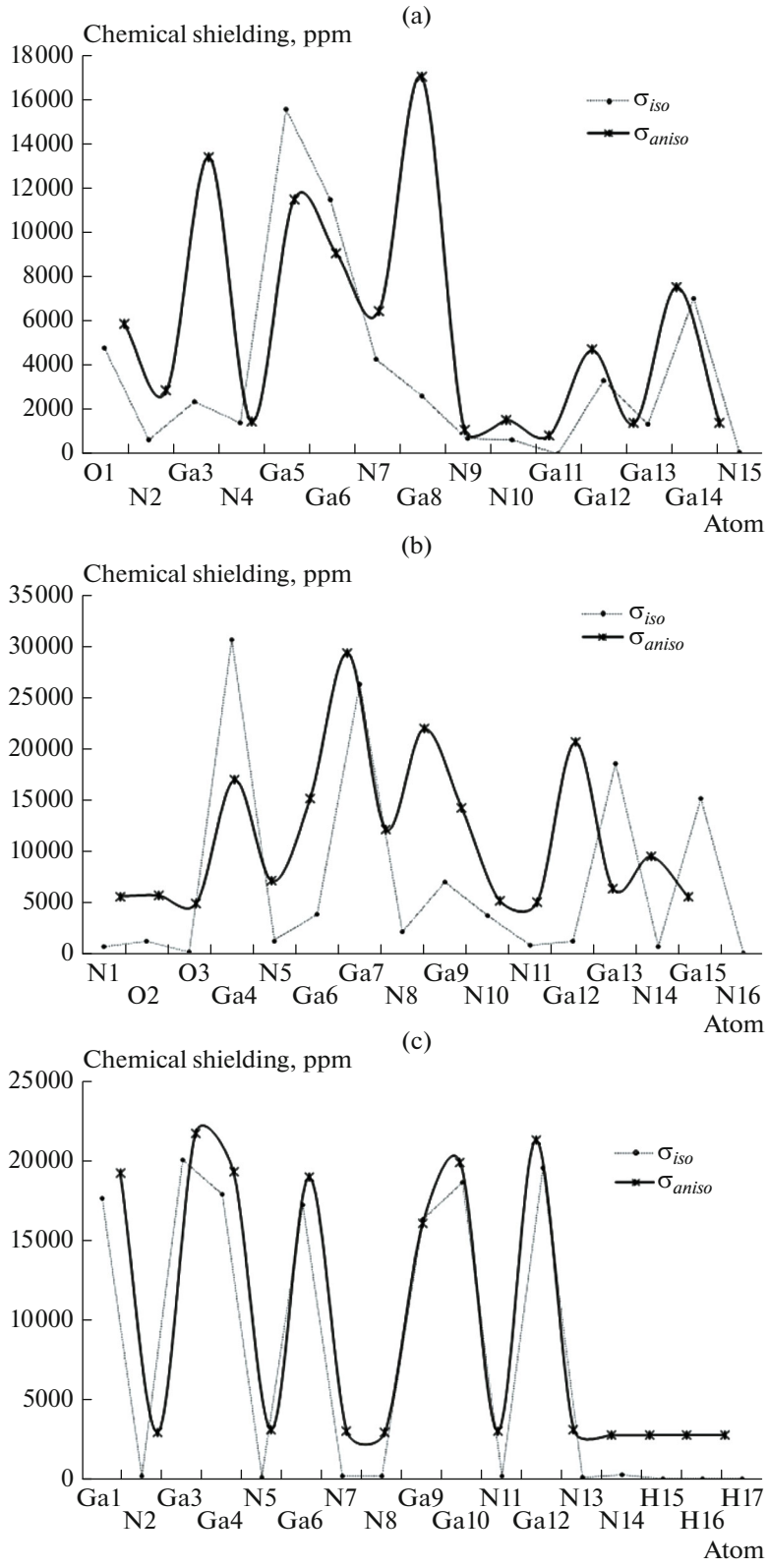

Fig. 4. "NMR" adsorbing of NO, NO_2, NH_3 on the GaN nanosheet (Fig. 1) through production of clusters of (a) NO → GaN, (b) NO_2 → GaN, and (c) NH_3 → GaN.

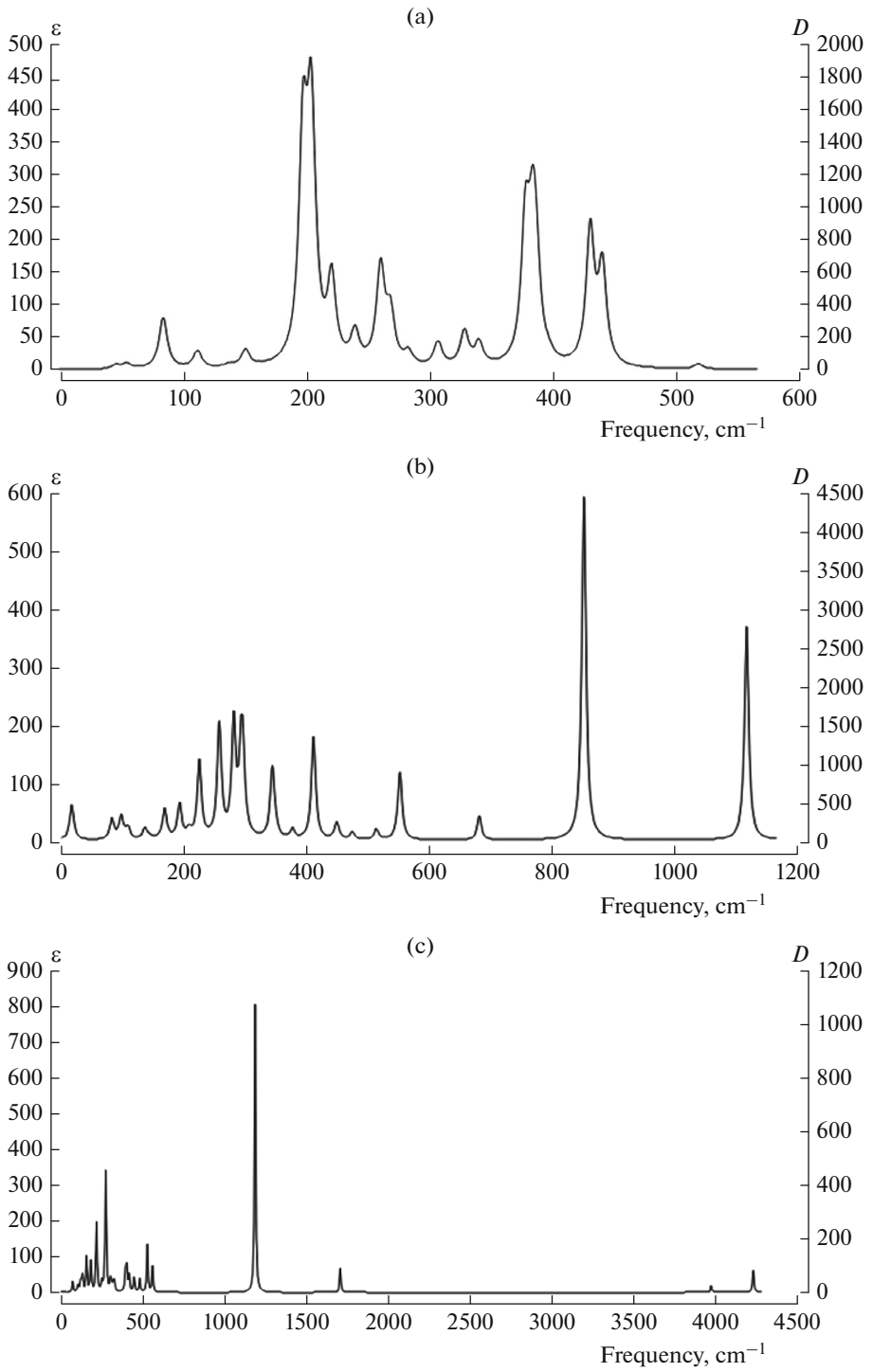

Fig. 5. The frequency (cm^{-1}) changes through the "IR" spectrums for (a) NO → GaN, (b) NO_2 → GaN, and (c) NH_3 → GaN nanosheets as the selective gas detectors.

GaN nanosheet (Table 4). In fact, it has been declared that "μ" shows chemical potential accompanying negative worth using B3LYP/LANL2DZ, 6-311+G(*d*, *p*), has an agreeable yield for capturing NO, NO_2, and NH_3 by GaN nanosheet (Table 4).

The illustration of donor–acceptor molecules depends on the relative frontier molecular levels. The HOMO–LUMO gap defines the charge transfer in gas molecules adsorbed on the GaN surface through simplified molecular-level diagram. In fact, the amount

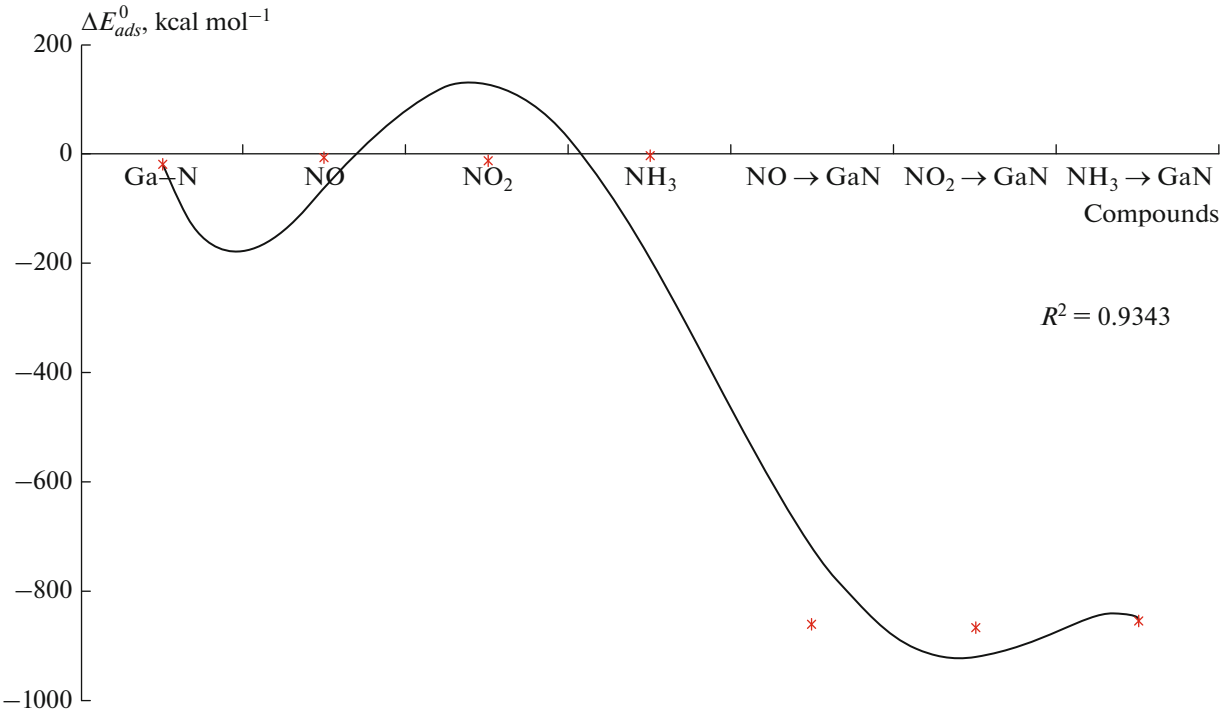

Fig. 6. The alterations of relative adsorption energy (ΔE^0_{ads}) for NO, NO_2, and NH_3 adsorbed on the surfaces of GaN nanosheet.

of transferred charges might be considerably small, as in the case of parallel and perpendicular coordination, which indicate electronic couplings smaller than in co-facial coordination. The results in Table 4 have indicated the energy level shifts of gas molecule → surface-HOMO and gas molecule → surface-LUMO of nanoclusters as a function of their distance *d* orbitals from the high symmetry points of each gas molecule on the GaN surface. Therefore, the HOMO level of molecule is being lowered as it loses its electron, whereas the LUMO level of surface is being raised as it gains partial charge.

Table 4. LUMO (a.u.), HOMO (a.u.), band energy gap (ΔE (eV)) and other quantities (eV) distributions of NO, NO_2, and NH_3 adsorbed on the surface of GaN nanosheet

Gas → GaN	LUMO	HOMO	ΔE	μ	χ	η	ζ	ψ
NO → GaN	 0.0447	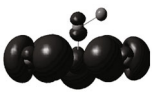 −0.0868	3.5783	−0.5733	0.5733	1.7891	0.2794	0.3888
NO_2 → GaN	 0.0257	 −0.1157	3.8496	−1.2235	1.2235	1.9248	0.2597	0.0918
NH_3 → GaN	 −0.0658	 −0.1486	2.2552	−2.9176	2.9176	1.1276	0.4434	3.7745

Band energy gap: $\Delta E = E_{LUMO} - E_{HOMO}$; chemical potential: $\mu = (E_{HOMO} + E_{LUMO})/2$; electronegativity: $\chi = -(E_{HOMO} + E_{LUMO})/2$; hardness: $\eta = (E_{LUMO} - E_{HOMO})/2$; softness: $\zeta = 1/(2\eta)$; electrophilicity index: $\psi = \mu^2/(2\eta)$.

CONCLUSIONS

The current research wanted to remark the illustration of gas adsorption on GaN nanosheet. Particularly, the structural, energetic, and infrared adsorption properties of linearly "atop" for NO, NO_2 and NH_3 molecules adsorbing on GaN nanosheet has been explored by using DFT calculations.

The values of changes of charge density have shown a more important charge transfer for GaN which acts as the electron acceptor while gas molecules act as the stronger electron donors through adsorption on the graphitic-like GaN surface. It has been assumed that the priority for selecting the surface binding of N-atom of NO, NH_3 and O-atom of NO_2 in adsorption site can be impacted by the existence of close atoms in the GaN surface.

In fact, Ga sites in GaN nanosheet have higher interaction energy from Van der Waals' forces with gas molecules including NO, NO_2 and NH_3 that can make them highly stable. Finally, our molecular simulation consequences have exhibited the existence of orbital hybridization between gallium sites and gas molecules of NO, NO_2 and NH_3 that also approves the recovery of adsorption susceptibility of graphene sheet. In fact, GaN nanosheet can promise an applicable outlook in the field of NO, NO_2 and NH_3 gas sensor.

Moreover, a thermodynamic formalism describing adsorption processes of gas molecules of NO, NO_2 and NH_3 on the solid adsorbent of GaN nanosheet has been developed. Besides, this process being treated as internal process of the adsorbent–adsorbate system. Thermodynamic parameters have constructed a detailed molecular model for atom–atom interactions and a distribution of point charges is used to reproduce the polarity of the solid material and the adsorbing molecules.

ACKNOWLEDGMENTS

In successfully completing this paper and its research, the authors are grateful to Kastamonu University for their support through the office, library, and scientific websites.

CONFLICT OF INTEREST

The authors declare that they have no conflicts of interest.

REFERENCES

1. L. Mahdavian, M. Monajjemi, M. Microelectron. J. **41**, 142 (2010). https://doi.org/10.1016/j.mejo.2010.01.011
2. F. Mollaamin, M. Monajjemi, Sensor Rev. (2023). https://doi.org/10.1108/SR-03-2023-0040
3. K. G. Bogolitsin, A. E. Parshina, N. V. Shkaeva, et al., Russ. J. Phys. Chem. B **15**, 1329 (2021). https://doi.org/10.1134/S1990793121080194
4. F. Mollaamin, M. Monajjemi, Molec. Simulation **49** (4), 365 (2023). https://doi.org/10.1080/08927022.2022.2159996
5. I. S. Golyak, D. R. Anfimov, I. B. Vintaykin, et al., Russ. J. Phys. Chem. B **17**, 320 (2023). https://doi.org/10.1134/S1990793123020264
6. M. M. Avilova, N. V. Zolotareva, O. V. Popova, Russ. J. Phys. Chem. B **17**, 329 (2023). https://doi.org/10.1134/S1990793123020203
7. A. E. Galashev, Russ. J. Phys. Chem. B **17**, 113 (2023). https://doi.org/10.1134/S1990793123010190
8. F. Mollaamin, M. Monajjemi, J. Mol. Model. **29**, 119 (2023). https://doi.org/10.1007/s00894-023-05526-3
9. D. Zhang, M. Ding, Y. Xu, et al., Russ. J. Phys. Chem. B **17**, 489 (2023). https://doi.org/10.1134/S1990793123020331
10. M. Islam, P. Ghosh, S. Karmaker, et al., Russ. J. Phys. Chem. B **15** (Suppl. 2), S189–S200 (2021). https://doi.org/10.1134/S1990793121100043
11. V. G. Lukin, O. G. Khvostenko, L. Z. Khatymova, et al., Russ. J. Phys. Chem. B **15**, 1008–1018 (2021). https://doi.org/10.1134/S1990793121060063
12. M. Pacheco, J. Pacheco, R. Valdivia, et al., MRS Adv. **2**, 2647 (2017).
13. G. V. Simbirtseva, S. D. Babenko, D. P. Kiryukhin, et al., Russ. J. Phys. Chem. B **17**, 107 (2023). https://doi.org/10.1134/S1990793123010116
14. F. Mollaamin, M. Monajjemi, J. Bio- Tribo-Corros. **9**, 47 (2023). https://doi.org/10.1007/s40735-023-00768-3
15. M. Khaleghian, M. Zahmatkesh, F. Mollaamin, et al., Full-Nanotub. Carbon Nanostruct. **19**, 251 (2011). https://doi.org/10.1080/15363831003721757
16. M. A. H. Khan, M. V. Rao, Q. Li, Sensors. **19**, 905 (2019). https://doi.org/10.3390/s19040905
17. F. Mollaamin, S. Shahriari, M. Monajjemi, et al., J. Clust. Sci. **34**, 1547 (2023). https://doi.org/10.1007/s10876-022-02335-1
18. A. Dey, Mater. Sci. Eng. B **229**, 206 (2018). https://doi.org/10.1016/j.mseb.2017.12.036
19. A. A. Eganov, D. A. Kardonsky, I. V. Sulimenkov, et al., Russ. J. Phys. Chem. B **17**, 503 (2023). . https://doi.org/10.1134/S1990793123020240
20. N. V. Dokhlikova, A. K. Gatin, S. Y. Sarvadiy, et al., Russ. J. Phys. Chem. B **16**, 361 (2022). https://doi.org/10.1134/S1990793122020166
21. M. Batmunkh, M. Bat-Erdene and J. G. Shapter, Adv. Mater. **28**, 8586 (2016)
22. T. Hussain, T. Kaewmaraya, S. Chakraborty, and R. Ahuja, J. Phys. Chem. C **120**, 25256 (2016)

23. N. V. Dokhlikova, S. A. Ozerin, S. V. Doronin, et al., Russ. J. Phys. Chem. B **16**, 461 (2022). https://doi.org/10.1134/S1990793122030137
24. X. Duan and C. M. Lieber, Adv. Mater. **12**, 298 (2000).
25. S. Shahriari, F. Mollaamin, and M. Monajjemi, Micromachines **14**, 241 (2023). https://doi.org/10.3390/mi14020241
26. Y. Ikawa, K. Lee, J.-P. Ao, et al., J. Appl. Phys. **53**, 114302 (2014).
27. F. Mollaamin, M. Monajjemi, J. Bio- Tribo-Corros. **9**, 33 (2023). https://doi.org/10.1007/s40735-023-00751-y
28. N. Prokopuk, K.-A. Son, T. George, et al., in *Proc. IEEE Sensors 2005, Irvine, CA, USA* (2005), p. 199.
29. S. J. Pearton, B. S. Kang, S. K. Kim, et al., J. Phys. Condens. Matter. **16**, R961 (2004).
30. M. A. Abdulsattar, Superlattices Microstruct. **93**, 163 (2016).
31. M. S. Khan and A. Srivastava, J. Electroanal. Chem. **775**, 243 (2016).
32. H. Cui, Y. Yong, H. Jiang, L. Yang, S. Wang, G. Zhang, M. Guo and X. Li, Mater. Res. Express **4**, 015009 (2017).
33. Y. Yong, H. Jiang, X. Li, S. Lv and J. Cao, Phys. Chem. Chem. Phys. **18**, 21431 (2016).
34. K. H. Baik, J. Kim and S. Jang, Sens. Actuators, B, **238**, 462 (2017).
35. Y. Yong, H. Cui, Q. Zhou, et al., RSC Adv. **7**, 51027 (2017). https://doi.org/10.1039/c7ra11106a
36. M. Monajjemi, H. Yamola, and F. Mollaamin, Fuller. Nanotub. Carbon Nanostructures **22** (6), 595 (2014). https://doi.org/10.1080/1536383X.2012.702163
37. M. Monajjemi, R. Faham, and F. Mollaamin, Fuller. Nanotub. Carbon Nanostructures **20** (2), 595 (2012). https://doi.org/10.1080/1536383X.2010.533310
38. H. Jalilian, M. Monajjemi, Jpn. J. Appl. Phys. **54**, 085101 (2015). https://doi.org/10.7567/JJAP.54.085101
39. T. Kente, S. D. Mhlanga, J. Cryst. Growth **444**, 55 (2016).
40. F. Mollaamin, M. Monajjemi, J. Mol. Model. **29**, 170 (2023). https://doi.org/10.1007/s00894-023-05567-8.41
41. N. Dural and M. V. Romalis, APL Materials **2** (8), (2014) https://doi.org/10.1063/1.4891375
42. K. Park, J. Lee, D. Kim, et al., ACS Omega. **4**, 2, 3098 (2019). https://doi.org/10.1021/acsomega.8b03548
43. M. Šetka, M. Claros, O. Chmela, et al., J. Mater. Chem. C **9**, 16804 (2021). https://doi.org/10.1039/D1TC04247E
44. X. Geng, X. Liu, L. Mawella-Vithanage, et al., ACS Sens. **6**, 4389 (2021). https://doi.org/10.1021/acssensors.1c01694
45. J. Shin, S. Han, S. Noh, et al., Nanotechnology **32**, 505201 (2021). https://doi.org/10.1088/1361-6528/ac2427
46. R. W. Pinder, J. T. Walker, J. O. Bash, et al., Geophys. Res. Lett. **38**, L04 802 (2011). https://doi.org/10.1029/2010GL046146
47. J. M. Langridge, D. Lack, C. A. Brock, et al., J. Geophys. Res. Atmos. **117**, D00v11 (2012). https://doi.org/10.1029/2011jd017116
48. J. F. Lamarque, G. Kyle, M. Meinshausen, et al., Clim. Chang. **109**, 191 (2011).
49. S. Bagheri, M. Monajjemi, A. Ziglari, et al., Russ. J. Phys. Chem. B **15** (Suppl. 1), S140–(2021). https://doi.org/10.1134/S1990793121090049
50. O. N. Fedyaeva, A. V. Shishkin, and A. A. Vostrikov, Russ. J. Phys. Chem. B **16**, 1285 (2022). https://doi.org/10.1134/S1990793122070053
51. X. Miao, S. Zhou, and C. Wang, Russ. J. Phys. Chem. B **16**, 804 (2022). https://doi.org/10.1134/S199079312204011X
52. N. V. Dokhlikova, A. K. Gatin, S. Y. Sarvadiy, et al., Russ. J. Phys. Chem. B **16**, 772 (2022). https://doi.org/10.1134/S1990793122040042
53. R. Dennington, T. A. Keith, and J. M. Millam, *GaussView. Version 6* (Semichem Inc., Shawnee Mission, KS, 2016).
54. M. J. Frisch, G. W. Trucks, H. B. Schlegel, et al., *Gaussian 16, Revision C.01* (Gaussian, Inc., Wallingford CT, 2016).
55. J. P. Perdew, K. Burke, and M. Ernzerhof, "Generalized gradient approximation made simple," Phys. Rev. Lett. **77**, 3865 (1996).
56. G. Henkelman, A. Arnaldsson, and H. Jónsson, Comput. Mater. Sci. **36** (3), 354 (2006).
57. Y. G. Zhou, X. T. Zu, F. Gao, et al., J. Appl. Phys. **105** (10), 104311 (2009).
58. Y. Mao, J. Yuan, and J. Zhong, J. Phys.: Condens. Matter **20** (11), 115209 (2008).
59. D. A. H. Hanaor, M. Ghadiri, W. Chrzanowski, et al., Langmuir **30** (50), 15143 (2014). https://doi.org/10.1021/la503581e
60. A. Boyd, I. Dube, G. Fedorov, et al., Carbon **69**, 417 (2014).
61. F. Mollaamin and M. Monajjemi, J. Clust. Sci. (2023).
62. E. M. Sarasia, S. Afsharnezhad, B. Honarparvar, et al., Phys. Chem. Liq. **49**, 561 (2011). https://doi.org/10.1080/00319101003698992
63. B. Ghalandari, M. Monajjemi, and F. Mollaamin, J. Comput. Theor. Nanosci. **8**, 1212 (2011). https://doi.org/10.1166/jctn.2011.1801

64. B. Khalili Hadad, F. Mollaamin, and M. Monajjemi, Russ. Chem. Bull. **60**, 238 (2011). https://doi.org/10.1007/s11172-011-0039-5

65. A. S. Arzumanyan, N. G. Amirkhanyan, Y. G. Grigoryan, et al., Russ. J. Phys. Chem. B **17**, 122 (2023). https://doi.org/10.1134/S1990793123010177

66. M. Monajjemi and F. Mollaamin, J. Comput. Theor. Nanosci. **9**, 2208 (2012). https://doi.org/10.1166/jctn.2012.2640

67. M. Monajjemi, H. Baheri, and F. Mollaamin, J. Struct. Chem. **52**, 54 (2011). https://doi.org/10.1134/S0022476611010070

68. M. A. A. Zadeh, H. Lari, L. Kharghanian, et al., J. Comput. Theor. Nanosci. **12**, 4358 (2015). https://doi.org/10.1166/jctn.2015.4366

69. K. Bakhshi, F.Mollaamin, and M. Monajjemi, J. Comput. Theor. Nanosci. **8**, 763 (2011). https://doi.org/10.1166/jctn.2011.1750

70. M. Monajjemi, M. Khaleghian, N. Tadayonpour, et al., Int. J. Nanosci. **9**, 517 (2010). https://doi.org/10.1142/s0219581x10007071

71. F. Mollaamin, A.R. Ilkhani, N. Sakhaei, et al., J. Comput. Theor. Nanosci. **12**, 3148 (2015). https://doi.org/10.1166/jctn.2015.4092

72. M. Monajjemi, V.S. Lee, M. Khaleghian, et al., J. Phys. Chem. C. **114**, 15315 (2010).

73. A. Tahan, F.Mollaamin, and M. Monajjemi, Russ. J. Phys. Chem. A **83**, 587 (2009). https://doi.org/10.1134/s003602440904013x

74. M. Monajjemi, F. Mollaamin, S. Shojaei, Biointerface Res. Appl. Chem. Biointerface Res. Appl. Chem. **10** (3), 5575 (2020). https://doi.org/10.33263/BRIAC103.575585

75. M. Monajjemi, M. T. Baie, F. Mollaamin, Russ. Chem. Bull. **59**, 886 (2010). https://doi.org/10.1007/s11172-010-0181-5

76. F. Mollaamin, M. Monajjemi, S. Salemi, et al., Fuller. Nanotub. Carbon Nanostruct. **19**, 182 (2011). https://doi.org/10.1080/15363831003782932